Trivalent Boron as an Acceptor in Donor–π–Acceptor-Type Compounds for Single- and Two-Photon Excited Fluorescence

Zhi-qiang Liu,[a] Qi Fang,*[a] Dong Wang,[a] Du-xia Cao,[a] Gang Xue,[a] Wen-tao Yu,[a] and Hong Lei[b]

Abstract: The synthesis, structure, and fluorescence properties of a series of new donor–π–acceptor (D–π–A) type compounds, with a trivalent boron, protected by two mesityl groups, as acceptor, and with various typical donors and different π-conjugated bridges, are reported. All these stable organoboron compounds show intense single-photon excited fluorescence (SPEF) and two-photon excited fluorescence (TPEF) in a wide spectral range from blue to green, with the spectral peak position of the SPEF being basically the same as that of the TPEF. The remarkably strong C–B(mesityl)$_2$ bonding, and the well-conjugated π-system, shown in X-ray crystal structures of two compounds, indicate some charge transfer features of the ground state. Meanwhile, spectral data indicate that the charge transfer from donor to acceptor is greatly enhanced in the excited states. Based on typical structural data and comprehensive spectral data, the following structure–property relationships can be drawn: 1) the moderate arylamino donor can more effectively enhance the SPEF and TPEF intensities than can the strong alkylamino donor; 2) stilbene is a better π-bridge than styrylthiophene for its capability of enhancing and blue-shifting the SPEF and TPEF of the corresponding D–π–A compounds; and 3) when compared to its boron-free precursors and other analogues, -B(mesityl)$_2$ invariably and consistently acts as an effective SPEF and TPEF fluorophore in all this series of organoboron compounds, which may result from its strong π-electron-withdrawing and charge transfer-inducing nature in the ground-state and, more dominantly, in the excited-state. Combining all the above positive structure factors, *trans*-4′-*N*,*N*-diphenylamino-4-dimesitylboryl-stilbene (compound **3**) stands out as the optimized green SPEF and TPEF emitter. This compound exhibits an SPEF quantum yield Φ of 0.91 at 522 nm in THF, a TPEF cross-section σ' that is an order of magnitude larger than that of its boron-free precursor upon excitation by 800 nm femto-second laser pulses, and a two-photon absorption section σ of 3.0×10^{-48} cm^4 s. In the blue light region, *trans*-4′-*N*-carbazolyl-4-dimesitylboryl-stilbene (compound **4**) shows significant SPEF and TPEF properties, with $\Phi = 0.79$ at 464 nm in THF and a large σ' value, which is five times that of fluorescein upon excitation by 740 nm femto-second laser pulses.

Keywords: boron · donor–acceptor systems · electron-deficient compounds · fluorescence

Introduction

When certain lasers are used as a pump source, some organic compounds can be excited by simultaneously absorbing two photons; the emission of frequency upconverted fluorescence may follow. Short-wavelength emission after long-wavelength excitation is the main characteristic of this so-called two-photon excited fluorescence (TPEF).[1] There are several advantages in the excitation process characterized by two-photon absorption (TPA), including intrinsically high three-dimensional resolution, high penetrating ability, and reduced photodamage. TPEF related photophysics and materials have attracted great research interest and have found applications in areas, such as three-dimensional optical data storage,[2] two-photon laser-scanning fluorescence microscopy,[3] and TPA-induced frequency upconverted lasing.[4] In recent years, the synthesis of various new compounds that exhibit large TPA and/or TPEF cross sections has greatly accelerated the development of two-photon science and technology.[5–10]

As we know, the TPA cross section σ is proportional to the imaginary part of the second-order hyperpolarizability,[1, 5] that is, TPA is associated with a third-order nonlinear optical process. One of the most effective molecular models for both second- and third-order nonlinear optical materials is the polar D–π–A model, in which the π-system is end-capped by an electron donor (D) and an electron acceptor (A). As

[a] Prof. Dr. Q. Fang, Dr. Z.-q. Liu, Dr. D. Wang, Dr. D.-x. Cao, Dr. G. Xue, Prof. W.-t. Yu
State Key Laboratory of Crystal Materials
Shandong University, Jinan, 250100 (China)
Fax(+86) 531-8564337
E-mail: fangqi@icm.sdu.edu.cn

[b] Prof. Dr. H. Lei
School of Information Science and Engineering
Shandong University, Jinan 250100 (China)

DOI: 10.1002/chem.200304833

trivalent nitrogen atom is isoelectronic with a carbanion, nitrogen-based electron donors have been widely adopted in molecular engineering for organic optoelectronics applications, including TPEF. Due to its vacant p_π orbital, three-coordinate boron is isoelectronic with a carbonium and should be capable of receiving part of a negative charge from an electron donor through certain π-conjugated bridges. Indeed, some reported experiments have revealed that the conjugation of the vacant p_π orbital on boron with the π-orbital of an attached π-conjugated moiety is responsible for some linear and nonlinear optical properties, such as single-photon excited fluorescence (SPEF),[11, 12] molecular second harmonic generation (SHG),[13, 14] and electroluminescence (EL).[15] However, the TPEF properties of compounds that contain trivalent boron have not previously been well investigated.

Unfortunately, most organoboron compounds are not stable in air, so some bulky groups must be attached to trivalent boron to protect it from attack by oxygen. Among various designs to protect boron(III), the adoption of a mesityl group (-Mes) has proved to be successful.[16, 17] Recently, we briefly reported the TPEF properties of several D–π–A type compounds with $-B(Mes)_2$ as the electron acceptor.[17] As part of our continuing work to develop trivalent organoboron compounds useful as TPEF compounds, we have systematically synthesized more D–π–A-type compounds with typical donors, including alkylamino and arylamino groups, and with different π-conjugated systems, such as stilbene or styrylthiophene (compounds **1**–**10**). In all these compounds, the

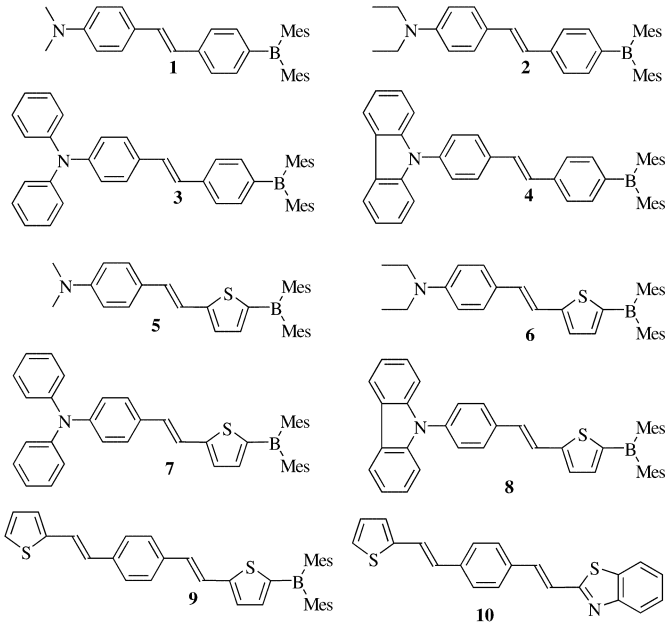

$-B(Mes)_2$ acceptor is retained, to allow evaluation of its effect on the TPEF properties. All the compounds show high fluorescence quantum yields and large TPA and TPEF cross sections, and the structure–property relationship has become much clearer. Here, we report in detail the synthesis and single- and two-photon related photophysical properties of these compounds.

Results and Discussion

Synthesis: As shown in Scheme 1, compounds **1′**–**9′**, as the precursors of compounds **1**–**9**, were synthesized by a modified Wittig reaction. Substitution of the 4′-bromine atom on the compounds **1′**–**4′** or the 5-H atom on the thienyl moiety of compounds **5′**–**9′** by a dimesitylboron group, in the presence of *n*-butyllithium at low temperature, affords normal yields of the target compounds **1**–**9**. The starting material **S-5**, a precursor of compound **10**, was prepared in a similar way to the literature method.[18] It is important to note that, if the *cis* isomer had not been isomerized to the *trans* isomer, the Wittig reaction would produce a mixture of the *trans*- and *cis*-alkenes. As a result, the $-B(Mes)_2$-substituted product would also be a mixture. To obtain the *trans*-conformation target compounds, which possess better photostability and fluorescence properties,[13] the isomerization of *cis* to *trans*-compounds is necessary. Pure products were characterized by NMR spectroscopy, MS, and elemental analysis (see the Experimental Section for details). All these organoboron compounds are stable in air in the solid state; they are even stable in dilute solutions. In fact, these compounds are long-lived in common organic solvents, which allows purification by, for example, recrystallization.

Structural studies: As shown in Figure 1 for compound **1**, the central boron and its three bonded carbon atoms are perfectly co-planar, forming a quasi-equilateral trigonal BC_3 plane

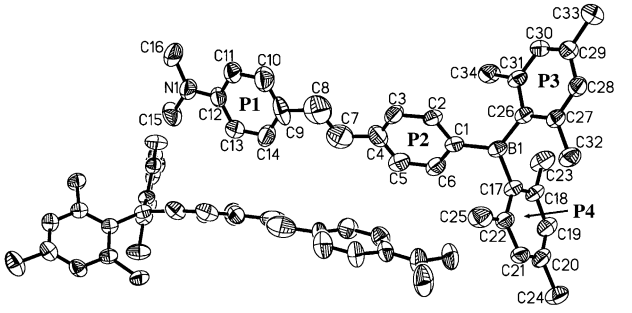

Figure 1. A pair of molecules of compound **1**, arranged perpendicularly, in a crystal.

(defined as the P0 plane). The deviations from the least-squares plane are: B1 0.0015, C1 −0.0005, C17 −0.0005, C26 −0.0005 Å. This indicates a sp^2 hybrid format for the atomic orbitals of the central boron. Around the central boron, three benzene ring planes (labeled P2, P3, and P4) are arranged in a propeller-like fashion, with the dihedral angles being 27.9(3)° (between P0 and P2), 43.3(3)° (between P0 and P3), and 66.7(3)° (between P0 and P4). Evidently, the four *o*-methyl moieties on the two mesityl groups play an important part in protecting the trivalent boron, with the minimum and maximum B···C distances being 2.97(1) (B, C23) and 3.08(1) Å (B, C32), respectively. The bond lengths of B1–C17 and B1–C26 are 1.566(6) and 1.572(6) Å, respectively. However, that of B1–C1 is reduced to 1.556(6) Å, indicating some additional π-bonding between trivalent boron and stilbene. At the N-based donor end, the central nitrogen

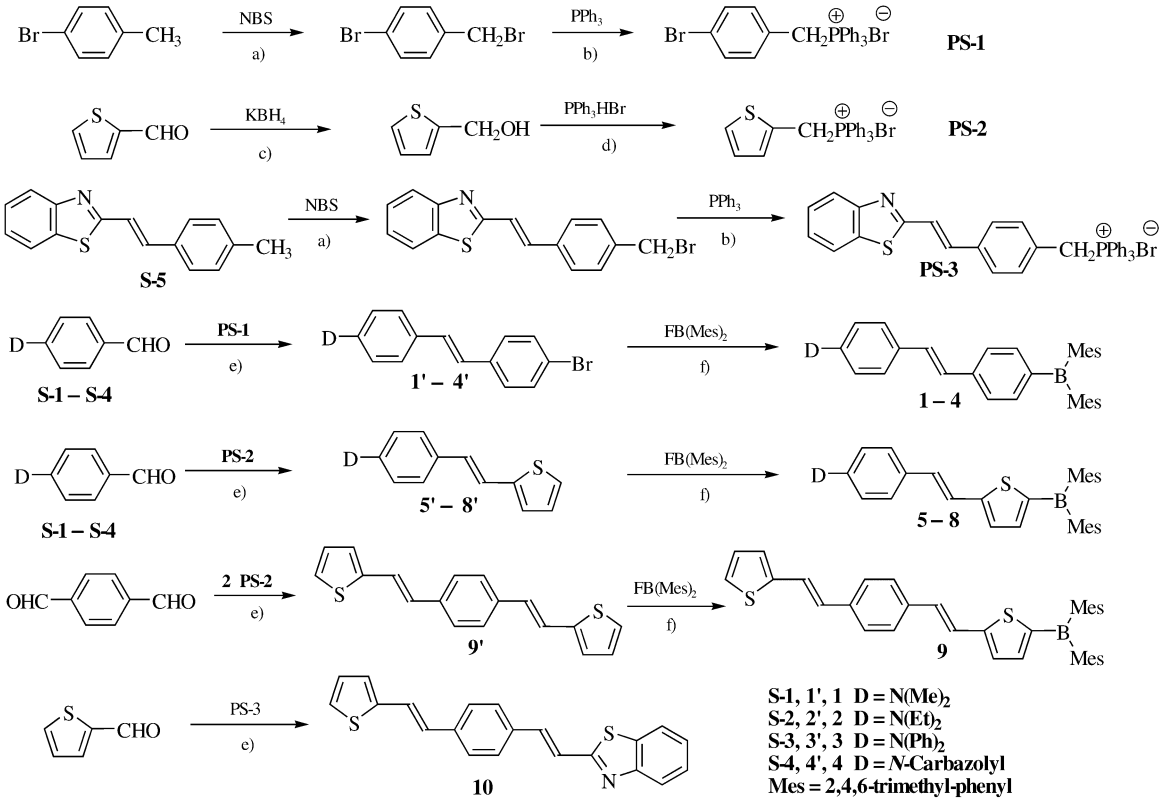

Scheme 1. Synthetic routes to compounds **1**–**10**. Reaction conditions: a) CCl_4, reflux, 4 h; b) toluene, reflux, 2 h; c) C_2H_5OH, reflux, 2 h; d) $CHCl_3$, reflux, 6 h; e) *t*BuOK, THF, 0 °C, 24 h; f) *n*-LiBu, THF, −78 °C – RT, 24 h.

and its three bonded carbon atoms are also perfectly co-planar and form a trigonal NC_3 plane, with the sum of the three C – N – C angles (359.8°) being very close to 360°. In fact, the entire aniline group is basically co-planar. This co-planarity of the trigonal NC_3 in compound **1** implies that the lone pair of electrons may be largely delocalized into the large π-system, even in the ground state. The conjugation of the stilbene is not perfect. There is a skew angle of 20.3(3)° between its two benzene rings (P1 and P2) and the linkage C9−C8=C7−C4 between P1 and P2 is not well conjugated (the bond lengths are: C4−C7 1.554(8), C7=C8 1.315(5), and C8−C9 1.525(8) Å). Two adjacent molecules in the crystal are oriented in a perpendicular and head-to-tail manner (shown in Figure 1).

Compound **5** shares much structural similarity with compound **1**, such as the perfect planarity of the quasi-equilateral trigonal conformation of the BC_3 acceptor and the NC_3 donor. As shown in Figure 2, two mesityl groups are also arranged in a propeller-like fashion, with the dihedral angles between the BC_3 plane (P0) and three neighboring aromatic-ring planes being 21.44(2)° (P0, P2), 59.30(2)° (P0, P3), and 57.20(2)° (P0, P4), respectively. Compared with **1**, compound **5** shows more charge-transfer features. As shown in Figure 2, the dihedral angle between the thiophene ring (P2) and the benzene ring (P1) is only 10.86°. The linkage between these two rings is quite conjugated, with bond lengths of 1.454(4) (C6−C9), 1.335(4) (C9=C10), and 1.443(4) Å (C10−C11). These suggest that all non-hydrogen atoms between nitrogen and boron are highly conjugated. The bond lengths of B1−C15 and B1−C24 are 1.571(5) Å and 1.585(4) Å, respectively, but that of

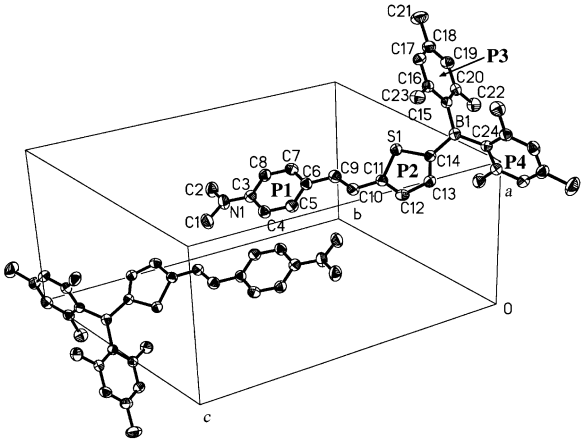

Figure 2. A pair of molecules of compound **5**, arranged parallel to each other, in the unit cell.

B1−C14 is substantially reduced to 1.544(5) Å. This remarkably strengthened B−C bonding, combined with the well-conjugated π-bridge, indicates some charge transfer in the ground state; thiophene may benefit this kind of charge transfer. In contrast to crystals of compound **1**, all molecules in crystals of compound **5** are packed in a parallel manner (also shown in Figure 2).

Linear absorption and single-photon excited fluorescence (SPEF): The photophysical data of the boron-containing compounds **1**–**9** and compound **10** in THF solutions are listed in Table 1, together with those of precursors **1′**–**9′** for comparison. All of these can be sorted by the π-conjugated

Table 1. Single- and two-photon-related photophysical properties of compounds **1**–**10** and **1′**–**9′** in THF solution.

	Single-photon-related properties[a]						Two-photon-related properties [b]		
	λ_{max}(abs) [nm][c]	λ_{max}(SPEF) [nm][d]	$10^{-3}\Delta\nu$ [cm^{-1}][e]	$10^{-3}m$ [cm^{-1}][f]	Φ[g]	τ [ns]	λ_{max}(TPEF) [nm]	σ [GM][h]	σ'[i]
1	403	538	6.28	13.38	0.55	1.95	540	188	3.2
2	414	540	5.64	11.94	0.60	1.89	541	194	3.6
3	402	522	5.72	13.95	0.91	2.15	520	300	8.3
4	359	464	6.30	12.85	0.79	1.84	466	212	5.1
5	431	558	5.28	11.32	0.35	1.60	559	74	0.8
6	444	566	4.86	9.59	0.35	1.64	564	93	1.0
7	428	536	4.71	12.03	0.82	2.18	540	119	3.0
8	397	484	4.53	11.17	0.84	1.95	484	123	3.2
9	417	500	3.98	9.49	0.65	1.50	505	239	4.8
10	380	473	5.17	8.52	0.50	1.00	477	111	1.7
1′	355	438	5.34	4.81	0.07	0.38			
2′	360	444	5.15	5.56	0.09	0.40			
3′	365	434	4.36	7.51	0.72	1.98	440	36	0.8
4′	340	412	5.32	5.87	0.44	1.19			
5′	361	436	4.69	4.70	0.10	0.51			
6′	371	440	4.54	4.88	0.12	0.41			
7′	374	442	4.11	7.56	0.54	1.81			
8′	345	417	5.01	6.04	0.38	1.03			
9′	370	447	4.66	0	0.10				

[a] Single-photon properties were measured at concentrations of 1.0×10^{-5} M L^{-1}. [b] Two-photon properties were measured at concentrations of 1.0×10^{-3} M L^{-1}. [c] Peak position of the longest absorption band. [d] Peak position of SPEF, excited at the absorption maximum. [e] Stokes-shift. [f] The slope of plots of $\Delta\nu$ versus Δf. [g] Quantum yields determined by using fluorescein as standard. [h] The TPA cross section; 1 GM = 10^{-50} cm^4 s $photon^{-1}$. [i] The relative value of TPEF emission cross-section by assigning that of fluorescein equal to 1.

bridges or by the donor and acceptor groups: stilbene-based **1**–**4** versus styrylthiophene-based **5**–**8**; alkylamino-ended **1**, **2**, **5**, and **6** versus arylamino-ended **3**, **4**, **7** and **8**; the dimesitylboryl-substituted compounds (**1**–**9**) versus their precursors (**1′**–**9′**).

Solvatochromism and photon-induced charge transfer: All the SPEF spectra of the organoboron compounds (**1**–**9**) show strong solvatochromism relative to those of their precursors (**1′**–**9′**). With increasing polarity of the solvent, their λ_{max} (SPEF) show remarkable bathochromic shifts. As shown in Figure 3, for example, λ_{max}(SPEF) of **3** is located at 476 nm in toluene and red-shifted to 574 nm in acetonitrile. In contrast, the shift of λ_{max}(abs) of the absorption spectra of **3** in acetonitrile, relative to that in toluene, is very limited (no more than 5 nm). Furthermore, with increasing polarity of the solvent, the fluorescence lifetimes of the compounds **1**–**9** are also increased. These results suggest that the molecular polarity of the fluorescent excited state (assumed to be the first excited state S_1) of these boron-containing compounds must be larger than that of the ground state, as the enhanced dipole–dipole interactions caused by increasing the polarity of solute and/or solvent will lead to a more significant energy-level decrease for the excited state.

The increase in the molecular dipole moment from the ground state to the excited state can be estimated by following the Lippert equation [Eqs. (1) and (2)]:[19]

$$\Delta\nu_{st}=\nu_{abs}-\nu_{SPEF}=2\Delta\mu_{eg}^2\Delta f/hca^3+\text{Const} \quad (1)$$

$$\Delta f=[(\varepsilon-1)/(2\varepsilon+1)]-[(n^2-1)/(2n^2+1)] \quad (2)$$

In Equation (1), $\Delta\nu_{st}$ is the Stokes' shift in wavenumber units, $\Delta\mu_{eg}$ is the difference in dipole moment between the excited state and the ground state, Δf is the so-called orientation polarizability, ε is the dielectric constant of the solvent, n is the refractive index of the solvent, and a is the cavity radius of the molecule.

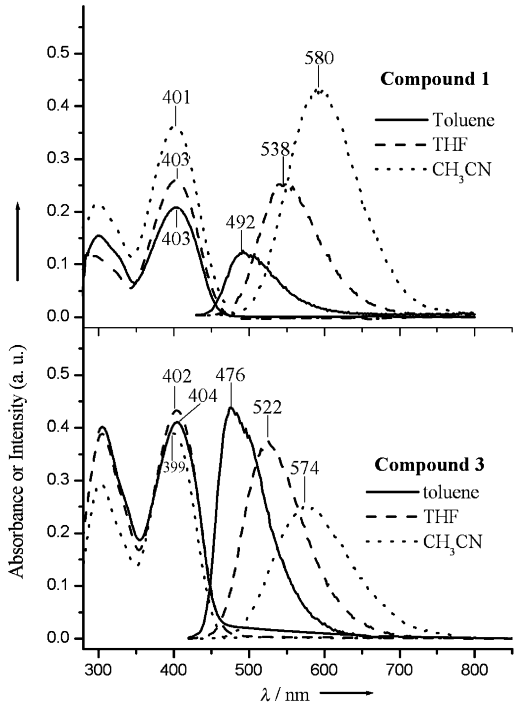

Figure 3. Linear absorption (left) spectra and SPEF spectra (right) of compounds **1** and **3** in three solvents, with $c=1.0\times10^{-5}$ mol L^{-1}.

The linearity between $\Delta\nu_{st}$ and Δf is quite good for all of the compounds **1**–**10** and **1′**–**9′**, and some plots of $\Delta\nu_{st}$ versus Δf are shown in Figure 4. According to Equation (1), the slope m of the fitted line of $\Delta\nu_{st}$ versus Δf will give the term $2\Delta\mu_{eg}^2/hca^3$. For a series of compounds with similar geometrical shape and size, the value of m is evidently a measure of $\Delta\mu_{eg}^2$. A much

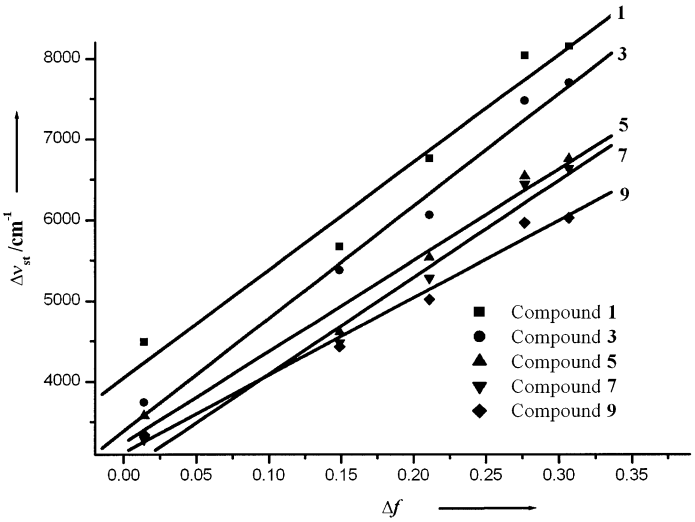

Figure 4. Stokes shift $\Delta\nu_{st}$ versus orientation polarizability Δf of the solvents.

larger value of m, that is, much larger solvatochromism, means a larger $\Delta\mu_{eg}$. As listed in the Table 1, most of the organoboron compounds show much larger m values than their boron-free precursors. Compound **3** shows the largest m value (13.95×10^3 cm^{-1}), which is about twice that of its boron-free precursor **3′** ($m = 7.51\times10^3$ cm^{-1}), while the m value of the non-polar compound **9′** was measured to be zero.

Comparison of the donors: There is only a small structural difference between compounds **1** and **2** and, accordingly, their spectroscopic differences are small. As shown in Table 1, the values λ_{max}(abs) and λ_{max}(SPEF) of **2** are red-shifted by 11 and 2 nm, respectively, relative to those of **1**, in THF. By replacing the dimethylamino with diphenylamino, the resultant compound **3**, also in THF, shows nearly the same λ_{max}(abs) value as **1**, but has a λ_{max}(SPEF) value that is blue-shifted by 16 nm, relative to that of **1**. The carbazolyl end-capped **4** shows such a tremendous spectral shift that its SPEF enters the blue-light range. The blue-shift of both λ_{max}(abs) and λ_{max}(SPEF) of this compound, relative to those of **1**, are 44 nm and 74 nm, respectively. In general, the values of both λ_{max}(abs) and λ_{max}(SPEF) show the sequence: **2** > **1** > **3** ≫ **4**. This spectral sequence may be in accordance with the sequence of electron-donating strength of the corresponding terminal amino group: diethylamino > dimethylamino > diphenylamino > carbazolyl. The diphenylamino group seems to be a weaker donor than the diethylamino group, due to the delocalization of the lone pair electrons of the N atom onto the terminal phenyl groups. The carbazolyl group, in which even greater delocalization occurs, seems to be a much weaker donor. This kind of delocalization in arylamino groups may have the effect of reducing the main flow of molecular charge transfer in the ground state.

The fluorescence quantum yields and lifetimes seem to be influenced not only by the donor's electron-donating ability, but also by its aromaticity. The replacement of the strong donor dimethylamino with the moderate donor diphenylamino results in a dramatically increased quantum yield and a moderately increased lifetime (**1** vs **3** and **5** vs **7** in Table 1). This may be attributed to larger delocalization of the lone pair electrons and, therefore, a larger molecular stabilization effect for the excited state of the aromatic arylamino groups.

Stilbene and styrylthiophene π-bridges: In our initial molecular design strategy, thiophene has been introduced because of its low stabilization energy, relative to benzene.[20] As a result, both the absorption and emission spectra of styrylthiophene-based compounds are considerably red-shifted, but, unexpectedly, their quantum yields are considerably less than those of their stilbene-based counterparts (**5** vs **1**, **6** vs **2**, **7** vs **3**, **8** vs **4** in Table 1). For example, the λ_{max}(abs) and λ_{max}(SPEF) values of compound **5** were red-shifted by 28 and 20 nm, respectively, relative to those of **1**, but the quantum yield of **5** was just 0.35 in THF (compared to 0.55 for **1**). The non-polar compound **9′**, which is symmetrically end-capped by two thienyl groups, shows very weak fluorescence, with a quantum yield of just 0.10. The Stokes' shifts and the m values of **5**, **6**, **7**, and **8** are evidently less than those of **1**, **2**, **3**, and **4**, respectively. Given that the molecular shape and volume of the styrylthiophene-based compounds **5**, **6**, **7**, and **8** are very close to those of the stilbene-based compounds **1**, **2**, **3**, and **4**, respectively, the dipole moment change $\Delta\mu_{eg}$ of the former compounds must, therefore, be smaller than those of the latter, respectively. Although the charge transfer of **1** seems less than that of **5** in the ground state, based on the crystalline data (comparing the B–C(P0) bond lengths and the planarity of the π-bridge of **1** with that of **5**), the charge transfer in the exited-state of **1**, **2**, **3**, and **4** may be much larger than that of **5**, **6**, **7**, and **8**, respectively, based on the above solvatochromism data. Therefore, replacement of benzene with thiophene has no positive effect in enhancing the fluorescence properties. The phenyl may still be a better aromatically π-conjugated unit to use, as the heavy sulfur atom in thiophene may enhance intersystem crossing or other non-radiation processes to quench fluorescence.

Boron-enhanced fluorescence and charge transfer: The Hammett substituent constant σ_H is a useful parameter for measuring the electron-withdrawing ability of an acceptor group. Glogowski and Willams have measured a value of $\sigma_{UV,H} = 0.65\pm0.03$ for a dimesitylboryl group, based on a spectroscopy correlation method.[21] From the absorption spectra data listed in Table 2, the σ_H sequence and the electron-withdrawing sequence of the acceptors seems to be: $-Br < -CN < -B(Mes)_2 < -NO_2$.

A direct comparison of the organoboron compounds **1**–**9** with their precursors **1′**–**9′** clearly indicates that the former group of compounds possess much improved photophysical properties. Firstly, **1**–**9** show fluorescence quantum yields and lifetimes that are a several times larger and longer, respectively, than those of **1′**–**9′** (shown in Table 1); this indicating that the $-B(Mes)_2$ group acts creditably as a fluorophore. Secondly, $-B(Mes)_2$ is an effective electron-withdrawing group that can act as an engine for charge transfer, especially in the excited-state. As listed in Table 1, the λ_{max}(abs) values of **1**–**9** are invariably red-shifted relative to **1′**–**9′**, respectively, with an average shift of 50.4 nm. Similarly, and more

Table 2. Photophysical properties of some related compounds.[a]

		λ_{max} (abs) [nm]	λ_{max} (SPEF) [nm]	Φ
11	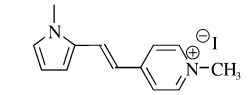	440	514	0.08
12	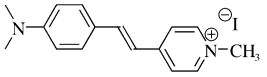	479	568	0.06
13	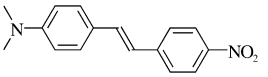	424	620	0.32
1	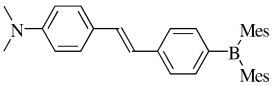	403	526	0.52
14	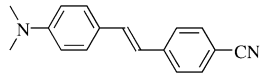	386	475	0.06
1'	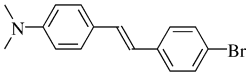	360	435	0.07

[a] All the data were re-measured in dioxane solution in our laboratory, except those of compound **14**, which are cited from ref. [23].

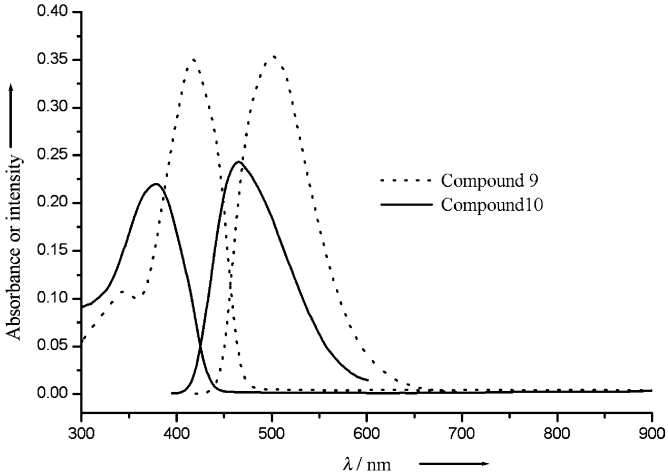

Figure 5. Linear absorption (left) and SPEF spectra (right) of compounds **9** and **10** in THF, with $c = 5.0 \times 10^{-6}$ mol L^{-1}.

remarkably, the λ_{max} (SPEF) of **1**–**9** are all red-shifted relative to **1′**–**9′**, respectively, with an average red-shift of 88.7 nm. Compounds **1**–**9** also have an average Stokes' shift of 5.25×10^3 cm^{-1}, an increase of 4.50×10^2 cm^{-1} relative to the corresponding average value for **1′**–**9′**. More generally, the average m value, interpreted to be $2\Delta\mu_{eg}^2/hca^3$ by Equation (1), of **1**–**9** is 11.75×10^3 cm^{-1}, which is twice that of the corresponding average for **1′**–**9′** (5.20×10^3 cm^{-1}). Given that the molecular volumes of **1**–**9** are much larger than their precursors **1′**–**9′**, respectively, the ratio of $\Delta\mu_{eg}^2$(**1**–**9**) to $\Delta\mu'^2_{eg}$(**1′**–**9′**) must be much larger than the ratio of m(**1**–**9**) to m'(**1′**–**9′**). At a conservative estimate, the dipole moment increase $\Delta\mu_{eg}$ of an organoboron compound (**1**–**9**) may be at least twice that of its precursor (**1′**–**9′**). Our comprehensive spectral data definitely indicate a much enhanced electron-withdrawing behavior of $-B(Mes)_2$ for the excited-state.

Comparison of the acceptors: We synthesized compound **10** as an analogue of **9** for a comparitive study, as 2-benzothiazolyl is also an electron acceptor.[22] Compared with **9′**, much improved SPEF properties, such as a higher quantum yield in **9** and **10**, should result from the introduction of the dimesitylboryl and 2-benzothiazolyl groups. As shown in Table 1, the λ_{max} (abs) value of **9** is red-shifted by about 30 nm, relative to **10**, in THF, and the m value of **9** is evidently larger than that of **10**. This indicates the stronger electron-withdrawing ability of dimesitylboryl in **9** compared with that of 2-benzothiazolyl in **10**. Additionally, the Hammett substituent constant of 2-benzothiazolyl ($\sigma_H = 0.29$[24]) is much smaller than that of dimesitylboryl. As shown in Figure 5, both the linear absorbance and the SPEF intensity of **9** are much stronger than that of **10** under the same experimental conditions. Clearly, **9** serves as a better fluorescence emitter than does **10**.

Quite similar to the issue about the donor-dependence of the fluorescence, the electron-accepting ability is not the only factor to influence the quantum yield. As revealed by the X-ray crystal structures of **1** and **5**, the trigonal BC_3 coordination plane is co-planar with the π-bridge and so is incorporated into the conjugate system; therefore, extended π-delocalization is another positive factor that enhances the SPEF properties. Furthermore, as shown in Table 2, compounds **13**, **14**, **1′**, and **1** possess the same electron donor and π-bridge, but the compound with the highest quantum yield is **1**, which contains the second-strongest acceptor $-B(Mes)_2$, rather than **13**, which contains the strongest acceptor. This may be due to the extra stabilization of the charge-separated excited state by the two aromatic mesityls on the $-B(Mes)_2$ group. Thus the electron-accepting ability, the extent of π-delocalization and this stabilization effect jointly make the trivalent-boron-based acceptor $-B(Mes)_2$ an excellent fluorescence activator.

Among all the object compounds and related analogues, compound **3** shows the best SPEF properties. This can be attributed to it combining all the optimized structural features: dimesitylboryl as acceptor, diphenylamino as donor, and stilbene as π-bridge. Following **3** comes the blue light emitter compound **4**, in which *N*-carbazolyl is the donor. Although the SPEF intensity and the quantum yield of **4** is inferior to that of **3**, the λ_{max} (SPEF) of **4** in THF is 464 nm, blue-shifted by 58 nm from the value of 522 nm exhibited by **3**.

Two-photon excited fluorescence: As shown in Figures 3, 5, and 8 (see later), which show some typical examples of linear absorption spectra, there is no detectable linear absorption in the wavelength range 600–1000 nm for any of the compounds mentioned in this paper. This means that there are no energy levels corresponding to an electron transition in this spectral range. If frequency upconverted fluorescence appears upon excitation with a tunable laser in this range, it should be mainly attributed to two-photon excited fluorescence (TPEF). To reduce the possibility of excited state absorption,[25] a femtosecond Ti:sapphire laser with the pulse width of 200 fs and the tunable range of 710–900 nm was adopted as the excitation source in our TPEF experiment.

TPEF spectra were recorded under the same experimental conditions, unless specially noted. Compounds **1**–**10** were excited at 800 nm except for **4**, which was excited at 740 nm. As shown in Table 1 and Figure 6, for a particular compound,

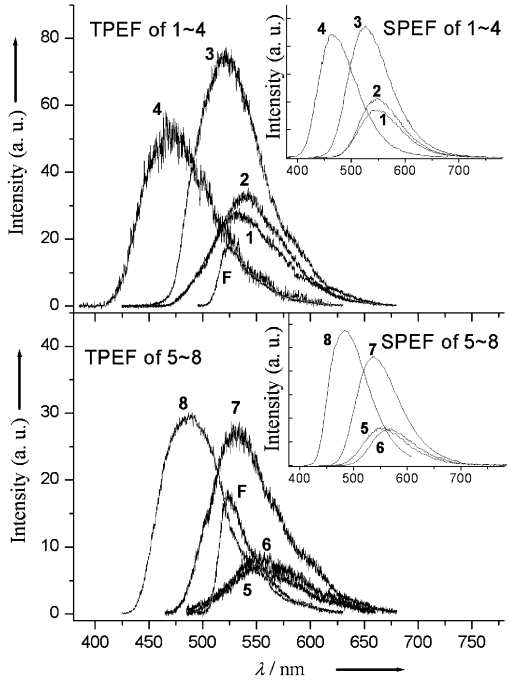

Figure 6. TPEF ($c = 1.0 \times 10^{-3}$ mol L^{-1}) and SPEF ($c = 1.0 \times 10^{-5}$ mol L^{-1}) spectra of compounds **1**–**8** in THF. **F** denotes fluorescein.

the spectral positions and profiles of SPEF and TPEF are basically the same. Most of our target compounds are stronger TPEF emitters than the fluorescein reference, and they show a TPEF intensity sequence that is the same as their SPEF intensity sequence. Considering all the similarities between SPEF and TPEF we can conclude that, although the molecules can be excited to different excited states by single-photon absorption or two-photon absorption, because of the different spectral selection rules, they would finally relax to the same fluorescent excited state. It seems certain that structural factors and environmental conditions that influence the SPEF properties of these compounds will similarly influence their TPEF properties, that is, the structural factors which positively or negatively influence the SPEF properties will also positively or negatively influence their TPEF properties.

Figure 7 shows a set of curves indicating the dependence of the output fluorescence intensity (I_{out}) on the input power (I_{in}), for compound **3**, compound **8**, and fluorescein (standard). These I_{out}/I_{in} curves fit well to the quadratic parabolas when the input laser power is not too high, indicating that the TPEF intensity is basically proportional to the square of the input laser intensity (this is the characteristic of the TPEF process[1]). When the input power is above a certain threshold, for example, 0.13 W for **3**, the quadratic-dependence begins to deviate, implying that some uncertain photophysical processes which cause fluorescence saturation are involved.

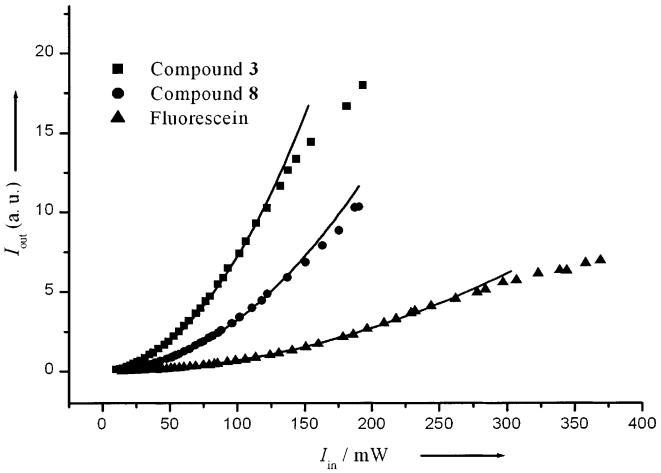

Figure 7. Dependence of output fluorescence intensity (I_{out}) on input laser power (I_{in}). Excitation carried out at 800 nm, with $c = 1.0 \times 10^{-3}$ mol L^{-1} in THF.

Detailed experiments demonstrate that the TPEF spectral peak position λ_{max}(TPEF) of our target compounds are independent of the excitation wavelength from 710 nm to 900 nm of the tunable laser, but the TPEF intensity evidently depends on this wavelength. By tuning the excitation wavelength with a step of 5 nm at a constant laser power, and recording the TPEF intensities, the two-photon excitation (TPE) spectra have been obtained, and those of compounds **1**, **5**, and **7** are shown in Figure 8. TPE spectra are relatively

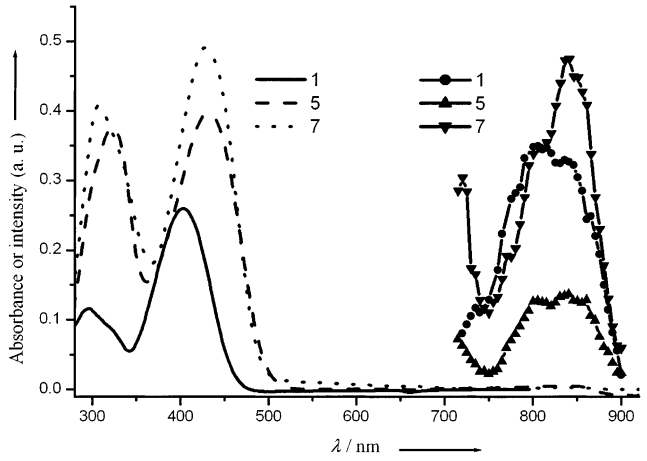

Figure 8. Linear absorption (left, with $c = 1.0 \times 10^{-5}$ mol L^{-1}) and two-photon excitation (right, with $c = 1.0 \times 10^{-3}$ mol L^{-1}) spectra of compounds **1**, **5**, and **7**.

easily obtained and less problematical than two-photon absorption (TPA) spectra. However, the TPE spectra may be similar to the TPA spectra and may be regarded as a sister of the latter. By comparing the single-photon absorption spectra (the solid-line graphs on the left of Figure 8) with the corresponding TPE spectra (the scattered-point graphs on the right of Figure 8), we can see that the linear absorption spectra and TPE spectra are similar, except that the latter is red-shifted to about twice of the wavelength of the former.

TPA cross-section and TPEF cross-section: TPA cross-section σ and TPEF cross-section σ' are fundamental parameters for TPA and/or TPEF materials. We adopted a TPEF-based method for measurement of σ and σ'. Fluorescein was selected as a reference in our experiment, as the σ values of several commercial dyes, such as fluorescein and rhodamine, have been carefully measured by Webb et al.[26, 27] and been used as reliable standards by several research groups.[7, 8] In addition, the emission range of fluorescein is similar to that of our samples.

The TPEF cross-section σ' values were measured by comparing their TPEF integral intensities F with that of fluorescein (F_{ref})under the same conditions, according to Equation (3):[26]

$$\sigma' = \sigma'_{ref}\frac{c_{ref}}{c}\frac{n_{ref}}{n}\frac{F}{F_{ref}} \quad (3)$$

The terms c and n are the concentration and refractive index of the sample/THF solution, respectively, and c_{ref} and n_{ref} are those of fluorescein. Compounds **4** and **3′** were excited at 740 nm and the others at 800 nm. All the measured σ' values of the target organoboron compounds, except that of **5**, are much larger than σ'_{ref} of fluorescein (shown in Table 1). By assigning $\sigma'_{ref} = 1$, compound **3** shows the largest relative σ' value of 8.3, which is an order of magnitude larger than that of its boron-free precursor **3′** (0.8).

The TPEF cross-section σ' parameters can be reasonably supposed to be proportional to the TPA cross-section σ parameters with the TPEF quantum yield Φ' as the proportion coefficient [Eq. (4)]:

$$\sigma' = \Phi'\sigma \quad (4)$$

By combining Equations (3) and (4), the expression for the σ can be obtained [Eq. (5)]:

$$\sigma = \sigma_{ref}\frac{\Phi'_{ref}}{\Phi'}\frac{c_{ref}}{c}\frac{n_{ref}}{n}\frac{F}{F_{ref}} \quad (5)$$

The TPEF quantum yield Φ' measurement is far more difficult, relative to the well-established SPEF quantum yield Φ measurement. One might suppose that $\Phi' = \Phi$, but this assumption is questionable. Although the fluorescent excited state (S_1 state) of TPEF can be supposed to be identical with that of SPEF, the relaxing processes from higher excited states to the S_1 state for TPEF and SPEF may be different. Another assumption [Eq. (6)] adopted in several reports may be better,[7, 8], as the error can be partly counteracted by the ratio effect. Therefore, Equation (5) becomes Equation (7).

$$\frac{\Phi'_{ref}}{\Phi'} = \frac{\Phi_{ref}}{\Phi} \quad (6)$$

$$\sigma = \sigma_{ref}\frac{\Phi'_{ref}}{\Phi}\frac{c_{ref}}{c}\frac{n_{ref}}{n}\frac{F}{F_{ref}} \quad (7)$$

In our experiments, the Φ_{ref} of fluorescein was taken to be 0.9,[28] and the laser power was kept at a constant 0.08 W for all samples. By assuming the σ_{ref} of fluorescein to be 36 GM ($1\ GM = 10^{-50}\ cm^4\,s\,photon^{-1}$),[27] the σ values for compounds **1**–**10** and precusor **3′** can be calculated and are listed in Table 1. Compound **3** again stood out as having the largest σ, 300 GM, which is about an order of magnitude higher than that of fluorescein and of its precursor **3′**.

It should be noted that the σ and σ' values have a sensitive dependence on the pulse width of the excitation laser. It has been reported that the σ' values measured with femtosecond laser pulses are orders of magnitude smaller than those measured with nanosecond laser pulses.[25] Compound **11** (in Table 2) has a similar emission region to our organoboron compounds and has been reported to exhibit upconverted green lasing when pumped by nanosecond laser at a high power level.[10] When excited by our femtosecond pulses, however, it shows much weaker TPEF intensities than those of our organoboron compounds under the same experimental conditions. In short, the TPEF results demonstrated that the $-B(Mes)_2$ acceptor group is not only an excellent SPEF activator, but is also an effective TPEF fluorophore.

Conclusion

In order to investigate the role of trivalent organoboron groups in linear SPEF and nonlinear TPEF materials, a series of stable donor–π–acceptor compounds with a $-B(Mes)_2$ acceptor group have been synthesized, along with analogues of these compounds for comparison studies. Comprehensive spectral data consistently demonstrate that the $-B(Mes)_2$ acceptor group is not only an excellent SPEF activator, but also an effective TPEF fluorophore in the blue-to-green optical region. The excellent SPEF and TPEF properties of these organoboron compounds can be attributed to the electron-withdrawing nature of trivalent boron in $-B(Mes)_2$; this causes some charge transfer in the ground state, a much enhanced charge transfer in the excited-state, and an extended π-delocalization. The mesityl group plays an important role in protecting the trivalent boron and in stabilizing the fluorescent excited state. The structural factors that positively or negatively influence the SPEF properties may also positively or negatively influence the TPEF properties of these organoboron compounds and related precursors. This work indicates that stable trivalent boron compounds are promising as two-photon-based materials.

Experimental

Synthesis and characterization: ^1H NMR spectra of the compounds were recorded on an INOVA-300 NMR Spectrometer. Electron impact (EI, 70 eV) mass spectra were obtained on an Agilent 5973N MSD Spectrometer. The melting points were measured on a METTLER-TOLEDO DSC822e differential scanning calorimeter at a heating rate of 20 °C min^{-1} under a nitrogen atmosphere. Elemental analyses were obtained on a PE 2400 autoanalyser.

2-Thiophenecarboxaldehyde was purchased from Acros. The starting materials 4-(*N*,*N*-diethylamino)benzaldehyde (**S-2**) and 4-(*N*-carbazolyl)-benzaldehyde (**S-3**) were synthesized by the literature method.[29] 4-(*N*,*N*-Diphenylamino)benzaldehyde (**S-4**) was prepared by the standard Vilsmeier reaction. Phosphonium salts (**PS-1**, **PS-2**, and **PS-3**) were prepared in our lab as shown in Scheme 1. Dimesitylboron fluoride ($BF(Mes)_2$) was purchased from Aldrich. Other reagents, such as 4-(*N*,*N*-dimethylamino)-benzaldehyde (**S-1**) and *p*-bromotoluene, were purchased from Shanghai Reagents. HPLC grade THF was freshly distilled with sodium-sand before use. All chemical reactions were carried out under a N_2 atmosphere. Our

synthetic strategy is outlined in Scheme 1 and the general procedures are described below.

General procedure of the Wittig reaction to give 1′–9′ and 10: The phosphonium salt (**PS-1**, **PS-2**, or **PS-3**, 1 equiv) and the aldehyde (**S-1**, **S-4**, or **S-6**, 1 equiv) were suspended in about freshly distilled THF (about 50 ml), then BuOK (1.2–1.5 equiv) in THF was added dropwise, with stirring. This procedure was carried out in an ice-bath. The mixture was continuously stirred at room temperature for a further 20 h, then poured into distilled water (200 ml). The pH value was adjusted to 7.0 by addition of 0.1M hydrochloric acid. The product was extracted twice with CH_2Cl_2, and the organic layer was dried overnight over anhydrous $MgSO_4$. The solvent was removed with a rotary evaporator to give the crude product. In order to get the desired *trans* compound, the crude product was isomerized by dissolving in toluene and refluxing with trace amounts of iodine for 4 h. After removing the solvent, the residue was purified by column chromatography on silica gel using chloroform-petroleum ether (1: 3) as eluent. Compound **9′** was synthesized with 1 equiv *p*-phthaldehyde and 2 equiv **PS-2** in a similar way.

General procedure for the organoboron compounds 1–9: *n*-Butyllithium (1.6M in hexane, 1.5 equiv) was added slowly into a suspension of the precursor (**1′–9′**, 1 equiv) in anhydrous THF at −78 °C. After one hour, the temperature was allowed to naturally rise to room temperature. Stirring was then continued for a further hour. The mixture was then cooled again to −78 °C and dimesitylboron fluoride (1 equiv in an appropriate quantity of THF) was added by injection. The solution turned dark green at once, then finally a clear fluorescent green. The mixture was stirred overnight without a cooling bath. All the solvents were removed under reduced pressure. The residue was hydrolyzed and the product was extracted with chloroform. The organic layer was separated, and the solvent was removed to give a viscous oil. This crude product was purified by column chromatography on silica gel using chloroform-petroleum ether (1: 5) as eluent.

***trans*-4′-*N*,*N*-Dimethylamino-4-dimesitylborylstilbene (1)**: Bright green sheet crystals. Yield 32%; m.p. 182–184 °C; ^{1}H NMR (300 MHz, $CDCl_3$, TMS): $\delta = 2.01$ (s, 12H; *o*-CH_3), 2.31 (s, 6H; *p*-CH_3), 3.08 (s, 6H), 6.82 (s, 4H; $C_6H_2Me_3$), 7.06–7.48 ppm (m, 12H); MS (70 eV, EI): *m*/*z* (%): 471 (100) [M^+]; elemental analysis calcd (%) for $C_{34}H_{38}BN$: C 86.61, H 8.12, N 2.97; found: C 85.97, H 8.23, N 2.81.

***trans*-4′-*N*,*N*-Diethylamino-4-dimesitylborylstilbene (2)**: Bright yellow powder. Yield 24%; m.p. 104–106 °C; ^{1}H NMR (300 MHz, $CDCl_3$, TMS): $\delta = 1.11$–1.26 (t, $J = 6.85$ Hz, 6H), 2.02 (s, 12H; *o*-CH_3), 2.31 (s, 6H; *p*-CH_3), 3.33–3.50 (q, $J = 6.82$ Hz, 4H), 6.83 (s, 4H; $C_6H_2Me_3$), 6.93–7.44 ppm (m, 12H); MS: *m*/*z* (%): 499 (100) [M^+]; elemental analysis calcd (%) for $C_{36}H_{42}BN$: C 86.56, H 8.47, N 2.80; found: C 86.25, H 7.97, N 2.61.

***trans*-4′-*N*,*N*-Diphenylamino-4-dimesitylborylstilbene (3)**: Green-yellow powder. Yield 46%; m.p. 176–178 °C; ^{1}H NMR (300 MHz, $CDCl_3$, TMS): $\delta = 2.03$ (s, 12H; *o*-CH_3), 2.31 (s, 6H; *p*-CH_3), 6.82 (s, 4H; $C_6H_2Me_3$), 6.98–7.47 ppm (m, 20H); MS: *m*/*z* (%): 595 (100) [M^+]; elemental analysis calcd (%) for $C_{44}H_{42}BN$: C 88.73, H 7.11, N 2.35; found: C 88.55, H 6.87, N 2.10.

***trans*-4′-*N*-Carbazolyl-4-dimesitylborylstilbene (4)**: Pale-green microcrystals. Yield 52%; m.p. 188–191 °C; ^{1}H NMR (300 MHz, $CDCl_3$, TMS): $\delta =$ 2.03 (s, 12H; *o*-CH_3), 2.31 (s, 6H; *p*-CH_3), 6.82 (s, 4H; $C_6H_2Me_3$), 7.20–7.59 (m, 16H), 8.08–8.18 ppm (d, $J = 6.34$ Hz, 2H); MS: *m*/*z* (%): 593 (100) [M^+], 473 (97) [M^+ – Mes]; elemental analysis calcd (%) for $C_{44}H_{40}BN$: C 89.03, H 6.79, N 2.36; found: C 88.83, H 6.71, N 2.17.

***trans*-2-[(4′-*N*,*N*-Dimethylamino)styryl]-5-dimesitylborylthiophene (5)**: Orange sheet crystals. Yield 42%; m.p. 163–164 °C; ^{1}H NMR (300 MHz, $CDCl_3$, TMS): $\delta = 2.14$ (s, 12H; *o*-CH_3), 2.30 (s, 6H; *p*-CH_3), 2.98 (s, 6H), 6.82 (s, 4H; $C_6H_2Me_3$), 6.95–7.36 ppm (m, 8H); MS: *m*/*z* (%): 477 (100) [M^+]; elemental analysis calcd (%) for $C_{32}H_{36}BNS$: C 80.49, H 7.60, N 2.93, S 6.71; found: C 79.87, H 7.77, N 2.99, S 7.11.

***trans*-2-[(4′-*N*,*N*-Diethylamino)styryl]-5-dimesitylboryl-thiophene (6)**: Orange sheet crystals. Yield 35%; m.p. 119–121 °C; ^{1}H NMR (300 MHz, $CDCl_3$, TMS): $\delta = 1.09$–1.25 (t, $J = 6.83$ Hz, 6H), 2.15 (s, 12H; *o*-CH_3), 2.31 (s, 6H; *p*-CH_3), 3.25–3.48 (q, $J = 6.82$ Hz, 4H), 6.83 (s, 4H; $C_6H_2Me_3$), 6.93–7.44 ppm (m, 8H); MS: *m*/*z* (%): 505 (100) [M^+]; elemental analysis calcd (%) for $C_{34}H_{40}BNS$: C 80.78, H 7.97, N 2.77, S 6.34; found: C 80.63, H 7.77, N 2.61, S 6.28.

***trans*-2-[(4′-*N*,*N*-Diphenylamino)styryl]-5-dimesitylborylthiophene (7)**: Yellow powder. Yield 51%; m.p. 179–182 °C; ^{1}H NMR (300 MHz, $CDCl_3$, TMS): $\delta = 2.15$ (s, 12H; *o*-CH_3), 2.31 (s, 6H; *p*-CH_3), 6.83 (s, 4H; $C_6H_2Me_3$), 6.95–7.36 ppm (m, 12H); MS: *m*/*z* (%): 601 (100) [M^+]; elemental analysis calcd (%) for $C_{42}H_{40}BNS$: C 83.85, H 6.70, N 2.33, S 5.33; found: C 82.90, H 6.66, N 2.02, S 5.30.

***trans*-2-[(4′-*N*-Carbazolyl)styryl]-5-dimesitylborylthiophene (8)**: Green sheet crystals. Yield 54%; m.p. 163–164 °C; ^{1}H NMR (300 MHz, $CDCl_3$, TMS): $\delta = 2.17$ (s, 12H; *o*-CH_3), 2.32 (s, 6H; *p*-CH_3), 6.85 (s, 4H; $C_6H_2Me_3$), 7.21–7.62 (m, 14H), 8.11–8.18 ppm (d, $J = 6.34$ Hz, 2H); MS: *m*/*z* (%): 599 (100) [M^+], 479 (43) [M^+ – Mes]; elemental analysis calcd (%) for $C_{42}H_{38}BNS$: C 84.13, H 6.39, N 2.34, S 5.35; found: C 84.02, H 6.34, N 2.10, S 5.30.

***trans*,*trans*-2-Dimesitylboron-5-{[4-(2-thiophene)ethenyl]styrene}thiophene (9)**: Yellow-green powder. Yield 35%; m.p. 205–207 °C; ^{1}H NMR (300 MHz, $CDCl_3$, TMS): $\delta = 2.14$ (s, 12H; *o*-CH_3), 2.31 (s, 6H; *p*-CH_3), 6.83 (s, 4H; $C_6H_2Me_3$), 7.03–7.19 (m, 9H), 7.42 ppm (s, 4H); MS: *m*/*z* (%): 542 (100) [M^+], 422 (26) [M^+ – Mes]; elemental analysis calcd (%) for $C_{36}H_{35}BS_2$: C 79.69, H 6.50, S 11.82; found: C 78.87, H 6.36, S 12.01.

***trans*,*trans*-2-{4-[2-(Thiophene-2-yl)ethenyl]styryl}1,3-benzothiazole (10)**: Yellow-green powder. Yield 38%; m.p. 240–241 °C; ^{1}H NMR (300 MHz, $CDCl_3$, TMS): $\delta = 6.90$–7.10 (m, 3H), 7.22–7.28 (m, 2H), 7.33–7.59 (m, 8H), 7.87 (d, $J = 7.8$ Hz, 1H), 8.01 ppm (d, $J = 7.8$ Hz, 1H); MS: *m*/*z* (%): 344 (100) [M^+]; elemental analysis calcd (%) for $C_{21}H_{15}NS_2$: C 73.01, H 4.38, N 4.05, S 18.56; found: C 72.69, H 4.29, N 4.13, S 18.44.

X-ray structural determinations: Single crystals of compounds **1** and **5** suitable for X-ray structure determination were obtained by slow evaporation of solution of these compounds in acetonitrile. X-ray diffraction data of **1** and **5** were collected on a Bruker Smart-1000 CCD diffractometer and a Bruker P4 four-circle diffractometer, respectively. Both of the radiation sources were $Mo_{K\alpha}$ ($\lambda = 0.71073$ Å). The crystal structures were solved by direct methods (SHELXL-97) and refined by full-matrix least-squares minimization on F^2. All non-hydrogen atoms were refined with anisotropic thermal parameters. The hydrogen atoms were

Table 3. Crystallographic data for compounds **1** and **5**.

	1	**5**
formula	$C_{34}H_{38}BN$	$C_{32}H_{36}BNS$
M_r	471.46	477.49
T [K]	298(2)	293(2)
crystal system	monoclinic	triclinic
space group	$P2_1/c$	$P\bar{1}$
a [Å]	8.411(3)	8.0588(12)
b [Å]	7.899(3)	10.4341(14)
c [Å]	43.847(14)	17.705(3)
α [°]	90	74.182(12)
β [°]	93.851(6)	86.993(9)
γ [°]	90	79.471(11)
V [Å^3]	2906.7(16)	1408.2(4)
Z	4	2
ρ_{calcd} [g cm^{-3}]	1.077	1.126
μ [mm^{-1}]	0.061	0.135
$F(000)$	1016	512
crystal size [mm^3]	0.50 × 0.40 × 0.10	0.44 × 0.40 × 0.05
θ range [°]	1.86–24.87	2.06–25.00
index range	$-9 \le h \le 9$	$-1 \le h \le 9$
	$-9 \le k \le 7$	$-11 \le k \le 11$
	$-51 \le l \le 50$	$-21 \le l \le 21$
reflections collected	13786	6043
reflections unique	4929	4905
R_{int}	0.0891	0.0259
data [$I > 2\sigma(I)$]	1397	2893
parameters	477	317
goodness-of-fit	0.893	1.140
$R1/wR^2$ [$I > 2\sigma(I)$]	0.0637/0.1305	0.0582/0.1602
$R1/wR^2$ (all data)	0.2175/0.1742	0.1084/0.1841
resd. min/max [e Å^{-3}]	−0.294/0.365	−0.225/0.274

Table 4. Selected bond lengths [Å] and angles [°].

Compound **1**			
B(1)−C(1)	1.556(6)	N(1)−C(16)	1.453(9)
B(1)−C(17)	1.566(6)	C(4)−C(7)	1.554(8)
B(1)−C(26)	1.572(6)	C(7)−C(8)	1.315(5)
N(1)−C(12)	1.373(6)	C(8)−C(9)	1.525(8)
N(1)−C(15)	1.451(7)		
C(1)-B(1)-C(17)	115.9(4)	C(3)-C(4)-C(7)	132.7(8)
C(1)-B(1)-C(26)	121.3(4)	C(8)-C(7)-C(4)	118.4(9)
C(17)-B(1)-C(26)	122.8(4)	C(7)-C(8)-C(9)	117.0(10)
C(12)-N(1)-C(15)	121.0(6)	C(10)-C(9)-C(14)	119.3(7)
C(12)-N(1)-C(16)	121.1(6)	C(10)-C(9)-C(8)	108.4(8)
C(15)-N(1)-C(16)	117.7(7)		
Compound **5**			
B(1)−C(14)	1.544(5)	C(6)−C(9)	1.454(4)
B(1)−C(15)	1.571(5)	C(9)−C(10)	1.335(4)
B(1)−C(24)	1.585(4)	C(10)−C(11)	1.443(4)
N(1)−C(3)	1.381(4)	C(11)−C(12)	1.368(4)
N(1)−C(2)	1.433(4)	C(12)−C(13)	1.405(4)
N(1)−C(1)	1.445(4)	C(13)−C(14)	1.360(4)
C(3)-N(1)-C(2)	121.0(3)	C(5)-C(6)-C(9)	123.1(3)
C(3)-N(1)-C(1)	120.8(3)	C(10)-C(9)-C(6)	128.5(3)
C(2)-N(1)-C(1)	118.3(3)	C(9)-C(10)-C(11)	126.3(3)
C(14)-B(1)-C(15)	118.1(3)	C(12)-C(11)-C(10)	126.5(3)
C(14)-B(1)-C(24)	115.5(3)	C(12)-C(11)-S(1)	109.8(2)
C(15)-B(1)-C(24)	126.4(3)	C(11)-C(12)-C(13)	113.3(3)
C(11)-S(1)-C(14)	93.31(15)	C(13)-C(14)-B(1)	129.4(3)

refined with a fixed isotropic thermal parameter related by a factor of 1.2 to the value of the equivalent isotropic parameter of their carrier atom. Weight factors were optimized in the final refinement cycles. For more information see Table 3. Some selected bond lengths and bonds angles are shown in Table 4. CCDC-190316 (compound **1**), and CCDC-203541 (compound **5**) contain the supplementary crystallographic data for this paper. These data can be obtained free of charge via www.ccdc.cam.ac.uk/conts/retrieving.html (or from the Cambridge Crystallographic Data Centre, 12 Union Road, Cambridge CB2 1EZ, UK; fax: (+44) 1223-336-033; or deposit@ccdc.cam.uk).

Optical measurements: All the solvents used for absorption spectra and fluorescence measurements were HPLC grade. For diluted solutions of $c = 1.0 \times 10^{-5}$ mol L^{-1}, in quartz cuvettes of 1 cm path length, linear absorption spectra were recorded on a PE lambda 35 UV-VIS spectrometer. Steady-state SPEF spectra and SPEF decay curves were recorded on an Edinburgh FLS920 fluorescence spectrometer equipped with a 450 W Xe lamp and a time-correlated single-photon-counting (TCSPC) card. All the SPEF spectra are corrected. Reconvolution fits of the decay profiles were made with F900 analysis software to obtain the lifetime values. To measure the quantum yields of these compounds, a 1.0×10^{-5} mol L^{-1} solution of fluorescein in 0.1 mol L^{-1} aqueous NaOH was used as the standard.[28]

For measurement of the TPEF emission spectra, TPEF excitation spectra and other TPEF properties, a Coherent Mira 900 femtosecond Ti:sapphire laser was used as a pump source, and a streak camera (Hamamatsu, model: C5680) in conjunction with an imaging spectrograph (Hamamatsu, model: C5094) was used as a recorder (see Figure 9). The laser beam was focused into the sample ($c = 1.0 \times 10^{-3}$ mol L^{-1}) by a lens. The frequency upconverted fluorescence was collected in a direction perpendicular to the pump beam. To minimize the re-absorption, the excitation beam was focused as closely as possible to the quartz cell wall, which faced the slit of the imaging spectrograph. The pulse width and repetition rate of the laser were 200 fs and 76 MHz, respectively.

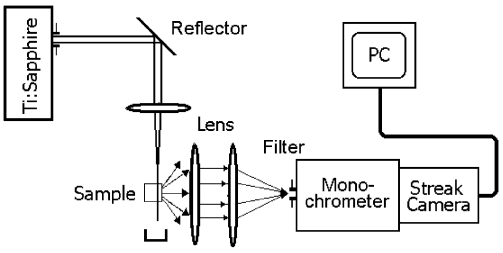

Figure 9. Experimental setup for TPEF measurement.

Acknowledgement

This work was supported by the National Natural Science Foundation of China (No. 20172034), the Foundation for University Key Teacher by the Ministry of Education, and a grant for State Key Program of China.

[1] J. D. Bhawalkar, G. S. He, P. N. Prasad, *Rep. Prog. Phys.* **1996**, *59*, 1041.
[2] a) D. A. Parthenopoulos, P. M. Rentzepis, *Science* **1989**, *245*, 843; b) B. H. Cumpston, S. P. Ananthavel, S. Barlow, D. L. Dyer, J. E. Ehrlich, L. L. Erskine, A. A. Heikal, S. M. Kuebler, I.-Y. Sandy Lee, D. McCord-Maughon, J. Qin, H. Röckel, M. Rumi, X.-L. Wu, S. R. Marder, J. W. Perry, *Nature* **1999**, *398*, 51; c) K. D. Belfield, K. J. Schafer, *Chem. Mater.* **2002**, *14*, 3656; d) K. D. Belfield, Y. Liu, R. A. Negres, M. Fan, G. Pan, D. J. Hagan, F. E. Hernandez, *Chem. Mater.* **2002**, *14*, 3663.
[3] a) W. Denk, J. H. Strickler, W. W. Webb, *Science* **1990**, *248*, 73; b) R. H. Röckel , J. Cao, W. R. Zipfel, W. W. Webb, M. R. Hansen, *Science* **1997**, *276*, 2039; c) A. Diaspro, M. Robello, *J. Photochem. Photobiol. B* **2000**, *55*, 1; d) J. D. Bhawalkar, G. S. He, C.-K. Park, C. F. Zhao, G. Ruland, P. N. Prasad. *Opt. Commun.* **1996**, *124*, 33.
[4] a) G. S. He, C. F. Zhao, J. D. Bhawalkar, P. N. Prasad. *Appl. Phys. Lett.* **1995**, *67*, 3703; b) G. S. He, R. Signorini, P. N. Prasad. *Appl. Opt.* **1998**, *37*, 5720; c) M. Fakis, J. Polyzos, G. Tsigaridas, J. Parthenios, A. Fragos, V. Giannetas, P. Persephonis, J. Mikroyannidis. *Chem. Phys. Lett*. **2000**, *323*, 111; d) Y. Ren, Q. Fang, W. T. Yu, H. Lei, Y. P. Tian, M. H. Jiang, Q. C. Yang , T. C. W. Mak, *J. Mater. Chem.* **2000**, *10*, 2025; e) A. Abbotto, L. Beverina, R. Bozio, S. Bradamante, C. Ferrante, G. A. Pagani, R. Signorini, *Adv. Mater.* **2000**, *12*, 1963; f) X. J. Tang, L. Z. Wu, L. P. Zhang, C. H. Tung, *Chem. Phys. Lett.* **2002**, *356*, 573.
[5] a) M. Albota, D. Beljonne, J.-L. Brédas, J. E. Ehrlich, J.-Y. Fu, A. A. Heikal, S. E. Hess, T. Kogej, M. D. Levin, S. R. Marder, D. McCord-Maughon, J. W. Perry, H. Röckel, M. Rumi, G. Subramaniam, W. W. Webb, X.-L. Wu and C. Xu, *Science* **1998**, *281*, 1653; b) M. Rumi, J. E. Ehrlich, A. A. Heikal, J. W. Perry, S. Barlow, Z. Hu, D. McCord-Maughon, T. C. Parker, H. Röckel , S. Thayumanavan, S. R. Marder, D. Beljonne, J.-L. Brédas, *J. Am. Chem. Soc.* **2000**, *122*, 9500.
[6] a) B. A. Reinhardt, L. L. Brott, S. J. Clarson, A. G. Dillard, J. C. Bhatt, R. Kannan, L. Yuan, G. S. He, P. N. Prasad, *Chem. Mater.* **1998**, *10*, 1863; b) K. D. Belfield, D. J. Hagan, E. W. Van Stryland, K. J. Schafer, R. A. Negres, *Org. Lett.* **1999**, *1*. 1575; c) K. D. Belfield, K. J. Schafer, W. Mourad, B. A. Reinhardt, *J. Org. Chem.* **2000**, *65*, 4475.
[7] a) L. Ventelon, S. Charier, L. Moreaux, J. Mertz, M. Blanchard-Desce, *Angew. Chem.* **2001**, *113*, 2156; *Angew. Chem. Int. Ed.* **2001**, *40*, 2098; b) L. Ventelon, L. Moreaux, J. Mertz, M. Blanchard-Desce, *Chem. Commun*. **1999**, 2055.
[8] a) B. R.Cho, K. H. Son, S. H. Lee, Y.-S. Song, Y.-K. Lee, S.-J. Jeon, J. H. Choi, H. Lee, M. Cho, *J. Am. Chem. Soc.* **2001**, *123*, 10039; b) B. R. Cho, M. J. Piao, K. H. Son, S. H. Lee, S. J. Yoon, S.-J. Jeon, M. Cho, *Chem. Eur. J.* **2002**, *8*, 3907.
[9] O.-K. Kim, K.-S. Lee, H. Y.Woo, K.-S. Kim, G. S. He, J. Swiatkiewicz, P. N. Prasad, *Chem. Mater*. **2000**, *12*, 284.
[10] a) S.-J. Chung, K.-S. Kim, T.-C. Lin, G. S. He, J. Swiatkiewicz, P. N. Prasad, *J. Phys. Chem. B* **1999**, *103*, 10741; b) A. Adronov, J. M. J. Fréchet, G. S. He, K.-S. Kim, S.-J. Chung, J. Swiatkiewicz, P. N. Prasad, *Chem. Mater*. **2000**, *12*, 2838.
[11] J. C. Doty, B. Babb, P. J. Grisdale, M.Glogowski, J. L. R. Williams, *J. Organomet. Chem.* **1972**, *38*, 229.
[12] Z. Yuan, J. C. Collings, N. J. Taylor, T. B. Marder, C. Jardin, J.-F. Halet, *J. Solid State Chem*. **2000**, *154*, 5.
[13] M. Lequan, R. M. Lequan, K. Chane-Ching, A. C. Callier, *Adv. Mater. Opt. Electron.* **1992**, *1*, 243.
[14] C. D. Entwistle, T. B. Marder, *Angew. Chem.* **2002**, *114*, 3051; *Angew. Chem. Int. Ed.* **2002**, *41*, 2927.

[15] a) T. Noda and Y. Shirota, *J. Am. Chem. Soc.* **1998**, *120*, 9714; b) T. Noda, H. Ogawa, Y. Shirota, *Adv. Mater.* **1999**, *11*, 283; c) Y. Shirota, M. Kinoshita, T. Noda, K. Okumoto, T. Ohara, *J. Am. Chem. Soc.* **2000**, *122*, 11021.
[16] a) H. C. Brown and V. H. Donson, *J. Am. Chem. Soc.* **1973**, *79*, 2302; b) S. Yamaguchi, T. Shirasaka, K. Tamao, *Org. Lett.* **2000**, *2*, 4129; c) S. Yamaguchi, S. Akiyama, K. Tamao, *J. Am. Chem. Soc.* **2001**, *123*, 11372; d) S. Yamaguchi, S. Akiyama, K. Tamao, *J. Am. Chem. Soc.* **2000**, *122*, 6335.
[17] Z. Q. Liu, Q. Fang, D. Wang, G. Xue, W. T. Yu, Z. S. Shao, M. H. Jiang, *Chem. Commun.* **2002**, 2900
[18] U. Rose, *J. Heterocyclic Chem.* **1992**, *29*, 551
[19] Von E. Lippert, *Z. Electrochem.* **1957**, *61*, 962.
[20] G. W. Wheland, *Resonance in Organic Chemistry*, Wiley, New York, **1955**, p. 99.
[21] M. E. Glogowski, J. L. R. Williams, *J. Organomet. Chem.* **1981**, *218*, 137.
[22] R. Kannan, G. S. He, L. Yuan, F. Xu, P. N. Prasad, A. G. Dombroskie, B. A. Reinhardt, J. W. Baur, R. A. Vaia, L.-S. Tan, *Chem. Mater.* 2001, **13**, 1896.
[23] R. Lapouyade, A. Kuhn, J.-F. Letard, W. Rettig, *Chem. Phys. Lett.* **1993**, *208*, 48.
[24] C. Hansch, A. leo, R. W. Taft, *Chem. Rev.* **1991**, *91*, 165.
[25] a) J. W. Baur, M. D. Alexander, Jr., M. Banach, L. R. Denny, B. A. Reinhardt, R. A. Vaia, P. A. Fleitz, S. M. Kirkpatrick, *Chem. Mater.* **1999**, *11*, 2899; b) J. Swiatkiewicz, P. N. Prasad, B. A. Reinhardt, *Opt. Commun.* **1998**, *157*, 135.
[26] C. Xu, W. W. Webb, *J. Opt. Soc. Am. B* **1996**, *13*, 481.
[27] M. A. Albota, C. Xu, W. W. Webb, *Appl. Opt.* **1998**, *37*, 7352.
[28] J. N. Demas, G. A. Crosby, *J. Phys. Chem.* **1971**, *75*, 991.
[29] C. F. Zhao, C.-K. Park, P. N. Prasad, Y. Zhang, S. Ghosal, R. Burzynski, *Chem. Mater.* **1995**, *7*, 1237.

Received: February 11, 2003 [F4833]